Uludağ University Journal of The Faculty of Engineering, Vol. 31, No. 1, 2026 RESEARCH

DOI: 10.17482/uumfd.1779891

# ANALYZING THE MECHANICAL BEHAVIORS OF DENTAL MATERIALS UNDER THERMAL AND LOADING CONDITIONS USING FINITE ELEMENT MODELING

*Murat HORASAN*[*]
*Murat ŞENOL* [**]

Received: 08.09.2025; revised: 06.02.2026; accepted: 06.02.2026

**Abstract:** Choosing the right restorative material is crucial in prosthetic dental treatments. Zirconia, lithium disilicate porcelains, and leucite-reinforced feldspathic porcelains are popular options because of their strong mechanical properties and outstanding aesthetics. In this study, finite element analyses were conducted to examine how these materials behave mechanically under a 450N compression load, under varying thermal conditions (5 °C, 22 °C, and 70 °C), and under loading scenarios (distributed, combined, vertical, or angular). Zirconia exhibited the highest peak stresses, reaching a maximum principal stress value of 184.89 MPa under 70°C and 30° oblique loading. However, it maintained the highest safety margin, utilizing only 20.5% of its 900 MPa flexural strength. In contrast, it was observed that leucite-reinforced porcelain reached 78.3% of the 160 MPa strength under the same conditions, making it the material with the lowest safety margin. It was determined that extreme temperature (70 °C) and oblique loading (30°) were the primary causes of stress intensification. It was observed that combined loading significantly increased localized surface stress concentrations at the occlusal contact points and cervical margins.

**Keywords:** Angular loading, Dental crown, Dental materials, Finite element analysis, Loading conditions, Thermal stress

**Sonlu Elemanlar Modellemesi Kullanılarak Termal ve Yük Koşulları Altında Diş Malzemelerinin Mekanik Davranışlarının Analizi**

**Öz:** Protez diş tedavilerinde doğru restoratif malzeme seçimi çok önemlidir. Zirkonya, lityum disilikat porselenler ve lüsit takviyeli feldspatik porselenler, güçlü mekanik özellikleri ve olağanüstü estetik özellikleri nedeniyle popüler seçeneklerdir. Bu çalışmada, bu malzemelerin 450 N basma yükü, değişen termal koşullar (5 °C, 22 °C ve 70 °C) ve yükleme senaryoları (dağıtılmış, birleşik, dikey veya açısal) altında mekanik olarak nasıl davrandıklarını incelemek için sonlu elemanlar analizleri yapılmıştır. Zirkonya, 70°C ve 30° eğik yükleme altında 184,89 MPa'lık bir maksimum asal gerilme değerine ulaşarak en yüksek tepe gerilmelerini sergilemiştir. Bununla birlikte, 900 MPa eğilme mukavemetinin yalnızca %20,5'ini kullanarak en yüksek güvenlik aralığını korumuştur. Buna karşılık, lüsit takviyeli porselenin aynı koşullar altında 160 MPa'lık mukavemetin %78,3'üne ulaştığı ve bu nedenle en düşük güvenlik aralığına sahip malzeme olduğu görülmüştür. Aşırı sıcaklığın (70°C) ve eğik yüklemenin (30°) gerilme yoğunlaşmasının başlıca nedenleri olduğu anlaşılmıştır. Kombine yüklemenin, oklüzal temas noktaları ile servikal kenarlarda lokalize yüzey gerilme konsantrasyonlarını önemli ölçüde artırdığı gözlemlenmiştir.

**Anahtar Kelimeler:** Açısal yükleme, Diş kronu, Diş malzemeleri, Sonlu elemanlar analizi, Yükleme koşulları, Termal gerilme

[*] Department of Mechanical Engineering, Engineering Faculty, Aksaray University, Aksaray, TÜRKİYE
[**] Dentistry Faculty, Aksaray University, Aksaray, TÜRKİYE

Corresponding Author: Murat HORASAN (murathorasan@aksaray.edu.tr)

## 1. INTRODUCTION

In prosthetic dentistry, evaluating the physical properties of materials is vital for ensuring the clinical success of ceramic crown restorations. Numerous studies consistently demonstrate the effective use of finite element modeling for analyzing dental materials (Al-Maqtari et al., 2014; Di Francesco et al., 2025). Although various techniques are available for computational analyses, dental research mainly concentrates on examining the solid-state mechanical properties of materials (Al-Maqtari et al., 2014).

The durability features of dental materials are crucial for the long-term success of prosthetic restorations. In the dynamic oral environment, which experiences temperature changes from food and exposure to various physical and chemical agents, changes in the restorative material's structure are inevitable. These structural changes are usually studied under either in vivo or in vitro conditions (Valandro et al., 2008; Hannigan and Lynch, 2013). The challenges of patient follow-up and maintaining a stable environment often hinder the standardization of research results. On the other hand, laboratory-based in vitro studies have the advantage of controlled environmental conditions, leading to more consistent outcomes (Valandro et al., 2008). As computer technology advances, biomedical analyses traditionally performed in vitro can now be conducted through mathematical calculations in virtual settings (Miranda et al., 2025). In particular, Finite Element Analysis (FEA) is a useful computational tool that allows researchers to efficiently analyze the mechanical properties of materials (Trivedi, 2014; Lahoud et al., 2024; Di Francesco et al., 2025).

Choosing the right restorative material is the most crucial step in prosthetic dental treatments. Even with careful preparation of the oral environment, the risk of failure remains high if an unsuitable material is selected. Zirconia and lithium disilicate porcelains are widely used because of their excellent mechanical properties and outstanding aesthetics (Cuzic et al., 2025). While zirconia has excellent compressive strength, its aesthetic qualities are generally considered lower than those of lithium disilicate porcelains. As a result, its high compressive strength makes it beneficial for restorations in the back (posterior) area. However, despite its strength, there is a risk of micro-crack formation during phase changes and potential fracture in thin sections, which can negatively impact the success of the restoration (Miranda et al., 2025). On the other hand, lithium disilicate and leucite-reinforced feldspathic porcelains are mainly known for their better aesthetic qualities. They are ideal for restorations in the front (anterior) region, providing excellent color matching (Cuzic et al., 2025; Fehrenbach et al., 2025).

Literature reviews show varying success and failure rates for all-ceramic crowns (da Mota Fonseca et al., 2025). Because the oral environment is exposed to many external factors, multiple causes contribute to restoration failure. Conducting in vivo studies on dental materials poses significant challenges for researchers (Valandro et al., 2008). However, technological advancements, especially those that enable more precise and detailed mathematical calculations, have greatly simplified the simulation of the dynamic oral environment (Trivedi, 2014). This allows for a more thorough observation of the combined effects of temperature changes and applied forces on restorative materials (Gongal et al., 2023).

The aim of this study was to examine the mechanical behavior of three common dental ceramics (Lithium disilicate, zirconia, and leucite-reinforced feldspathic porcelain )under various thermal and mechanical conditions by using finite element modeling. This work also explores the effects of two loading methods: distributed loading and combined loading (a single force).

## 2. MATERIAL AND METHODS

This study assessed the mechanical behavior of three common dental ceramics (Lithium disilicate, zirconia, and leucite-reinforced feldspathic porcelain) under different thermal (5 °C, 22 °C, and 70°C) and mechanical (0° and 30° load angles) conditions using finite element analysis (Table 1). We examined two loading methods: distributed loading (90 N on five surfaces) and

combined loading (a single 450 N force) (Table 1). A previous study offers detailed data across different tooth positions, from incisors to molars. In young adults, the maximum bite force measured at premolars (P3, P4) ranged roughly from 130 N to 424 N, with some individuals exceeding 300 N, and a high-performing subject nearing 450 N. Therefore, we selected 450 N as the occlusal load for the finite element analysis (Edmonds et al., 2020).

**Table 1**. **Finite element analysis parameters employed in the study**

| Parameters | Levels |
|---|---|
| **Materials** | Lithium disilicate<br>Zirconia<br>Leucite-reinforced feldspathic porcelain |
| **Temperatures** | 5 °C<br>22 °C<br>70 °C |
| **Load angles** | 0° - vertical loading<br>30° - oblique loading |
| **Load conditions** | Applying a 450 N load by distributing it as 90 N loads to five surfaces.<br>Applying a load of 450 N to five surfaces as a single, combined force. |

The materials modeled were lithium disilicate, zirconia, and leucite-reinforced feldspathic porcelain. Temperatures of 5°C and 70°C were selected to assess thermal effects on dental crowns under compression. These temperatures were chosen because they realistically simulate cold and hot thermal stresses that dental materials encounter in the mouth. While 5 °C mimics cold stimuli such as ice water, ice cream, and cold beverages, 70 °C represents hot stimuli like coffee, tea, hot soups, or meals. Several studies support the use of 5 °C and 70 °C (or similar values) as representative thermal conditions in dental material testing (Ayatollahi et al., 2015; Marelli et al., 2015). Load angles of 0° and 30° assessed how vertical and angular loads affect the crowns' mechanical response. We compared the two loading scenarios: a distributed 90 N load on five surfaces and a single, combined 450 N force (Table 1).

### 2.1. Dental Crown Geometry Generation

The crown geometry was created by capturing an impression of the prepared left lower first premolar tooth using a 3Shape Trios 5 intraoral scanner. The crown design for this tooth was then developed with ExoCAD software, based on the digital impression. The three-dimensional geometry obtained was converted to .stl (stereolithography) format, which was later used for CNC machining. The .stl file was imported into ANSYS SpaceClaim to generate a solid model. The model was scaled to match the actual size of the prototype. For further work, the generated model was transferred to ANSYS Workbench, as shown in Figure 1.

### 2.2. Finite Element Modeling

10-Node quadratic three-dimensional tetrahedral meshes with an element count of 117133, following a convergence study (Table 2), were created on the solid geometry of the dental crown in ANSYS. The mesh convergence study was conducted to assess the sensitivity of the finite element results to element size. The initial element size of 0.7 mm corresponds to the default mesh generated by ANSYS for the given geometry and served as the baseline configuration. The mesh was subsequently refined to 0.6 mm, 0.5 mm, and 0.4 mm to evaluate convergence behavior. As shown in Table 2, both the maximum and minimum principal stresses exhibited only minor variations across this refinement range, indicating numerical convergence. Further mesh

refinement below 0.4 mm was not pursued, as it resulted in substantially increased computational cost without a significant improvement in result accuracy.

Linear elastic FE models were conducted in ANSYS using the elastic modulus, Poisson's ratio, and Coefficient of Thermal Expansion (CTE) of the dental crown (Table 3). The elastic moduli for lithium disilicate, zirconia, and leucite-reinforced feldspathic porcelain used in the FE analyses were assigned as 95.9 GPa (Al Mortadi et al., 2020), 210 GPa (Al Mortadi et al., 2020), and 58.18 GPa (Capobianco et al., 2023), respectively (Table 3). All elements of the dental crown made of lithium disilicate, zirconia, and leucite-reinforced feldspathic porcelain in the FE analyses were assigned Poisson's ratios of 0.23 (Al Mortadi et al., 2020), 0.32 (Al Mortadi et al., 2020), and 0.08 (Capobianco et al., 2023), respectively (Table 3). The CTEs for lithium disilicate, zirconia, and leucite-reinforced feldspathic porcelain used in the dental crown were assigned as $10.6 \times 10^{-6}\ K^{-1}$ (Zarone et al., 2019), $10.8 \times 10^{-6}\ K^{-1}$ (Sasany et al., 2021), and $17.5 \times 10^{-6}\ K^{-1}$ (https://ivodent.hu/__docs/775_d9ea1b27d845c2dd50ef19b4a86c1fdc.pdf), respectively (Table 3).

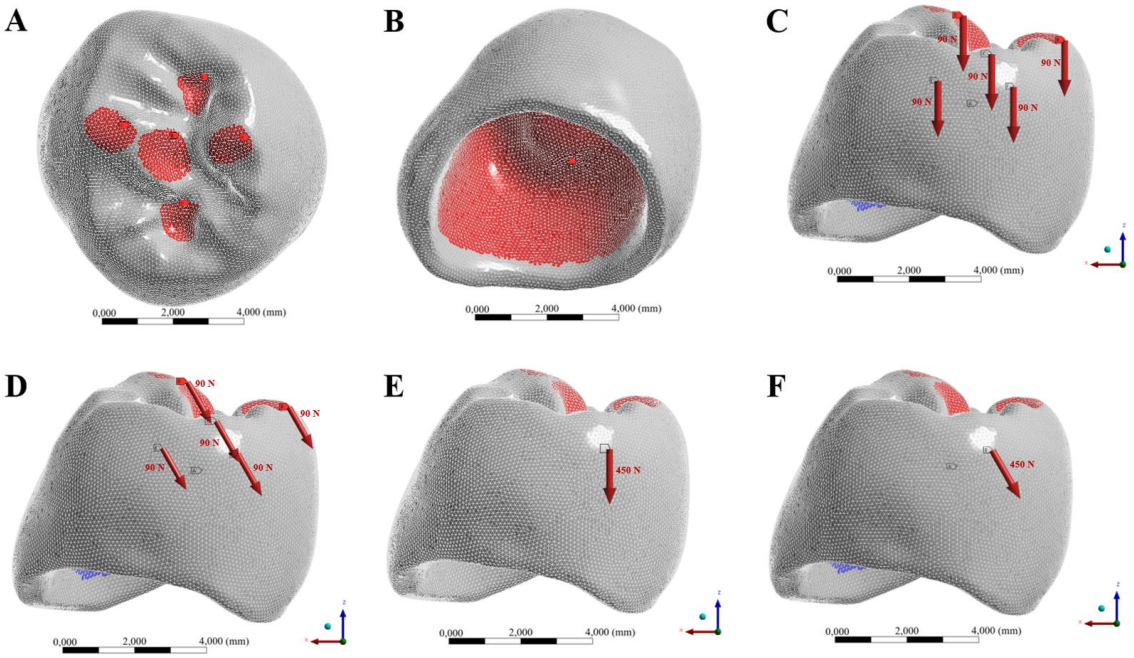


***Figure 1:***
*Boundary and loading conditions for the Finite Element Analyses:*
***A.*** *Occlusal contact areas* ***B.*** *Fixed area constrained against displacement and rotation in all directions* ***C.*** *Applying a 450 N load distributed as five 90 N loads at a 0° load angle on five surfaces* ***D.*** *Applying a 450 N load distributed as five 90 N loads at a 30° load angle on five surfaces* ***E*** *Applying a 450 N load at a 0° load angle to five surfaces as a single combined force.* ***F*** *Applying a 450 N load at a 30° load angle to five surfaces as a single combined force.*

The static structural finite element analysis was performed to simulate a compressive load test on the dental crown geometry for the left lower, first premolar tooth (Figure 1). Thermal effects were included through a sequentially coupled thermal–structural approach, in which a uniform temperature was applied as a thermal load to the structural model. Five occlusal contact areas were identified, as shown in Figure 1A, and the inner surface of the dental crown was constrained against displacement and rotation in all directions (Figure 1B). The occlusal load was

applied over five discrete contact areas located on the occlusal surface of the crown (Figure 1A). These regions correspond to clinically relevant cusp–fossa contact zones commonly engaged during functional mastication (Weinstein et al, 2025). Distributing the load across multiple contact areas enables a more physiologically realistic representation of occlusal loading compared with a single-point application, which may result in non-physiological stress concentrations (Benazzi et al, 2016).

**Table 2. Results of a mesh convergence study for finite element modeling of a representative molar tooth crown.**

| Maximum element size (mm) | Number of elements | Peak Max. Principal Stress (MPa) | Peak Min. Principal Stress (MPa) |
|---|---|---|---|
| 0.7 | 111051 | 125.43 | -181.55 |
| 0.6 | 111805 | 114.16 | -167.06 |
| 0.5 | 112983 | 108.74 | -157.22 |
| 0.4 | 117133 | 108.20 | -156.43 |

**Table 3. Mechanical properties used in the finite element model, including Young's modulus, Poisson's ratio, and the coefficient of thermal expansion (CTE) for the materials used in the molar tooth crown.**

| Material | Young Modulus [GPa] | Poisson's ratio | Coefficient of Thermal Expansion (CTE) [$K^{-1}$] | Flexural Strength (MPa) |
|---|---|---|---|---|
| Lithium disilicate | 95.9 | 0.23 | $10.6 \times 10^{-6}$ | 356.7 |
| Zirconia | 210 | 0.32 | $10.8 \times 10^{-6}$ | 900 |
| Leucite-reinforced feldspathic porcelain | 58.18 | 0.08 | $17.5 \times 10^{-6}$ | 160 |

The FE analyses were conducted using three common dental ceramics (lithium disilicate, zirconia, and leucite-reinforced feldspathic porcelain) under different thermal (5°C, 22°C and 70°C) and mechanical (0° and 30° load angles) conditions at two loading conditions: distributed loading (90 N on five surfaces) and combined loading (a single 450 N force) (Table 1). Thermal stress analyses examined dental crowns under compression at temperatures of 5°C, 22°C and 70°C. The temperature was set using a ramped load profile: starting at 22 °C at t = 0 s and then increasing linearly to 70 °C or decreasing to 5 °C by t = 1 s. In this context, t is the pseudo-time used for load ramping within a quasi-static structural analysis; no heat transfer equations were solved, so convection, radiation, or heat-flux boundary conditions were not applied. Thermal strains were calculated from the specified temperature variation using the material's coefficient of thermal expansion and combined with the mechanical load constraints.

Load angles of 0° and 30° were evaluated to understand how vertical and angular loads affect the mechanical response of the crowns (Fig 1C, D, E, F). Additionally, the effects of two loading scenarios -distributed loading (90 N applied on five surfaces) and combined loading (a single 450 N force)- were assessed (Fig 1C, D, E, F). The compressive load was applied at angles of 0° and 30° as either distributed or combined loads on the occlusal contact areas (Fig 1C, D, E, F). Peak

and average values of the maximum and minimum principal stresses were computed for the dental crown in all cases with varying materials, temperatures, and loading conditions.

## 3. RESULTS AND DISCUSSION

Peak and average values of the maximum and minimum principal stresses are assessed to understand stress concentration and distribution within the various dental crown materials under thermal and mechanical loading conditions (Table 4, Figures 2-5).

### 3.1. Influence of Loading Conditions

At the neutral baseline temperature of 22 °C, the loading mode exerted a distinct influence on the peak stress magnitudes, while the bulk stress of the restorations remained largely unaffected. A comparative analysis of the data in Table 4 reveals that the transition from a distributed 450 N load (applied as five separate 90 N forces) to a single combined 450 N force leads to a significant intensification of compressive stress, represented by the minimum principal stress. For instance, in the lithium disilicate crown under vertical loading (0°), the peak compressive stress increased from -158.38 MPa with distributed loading to -199.94 MPa under combined loading (Table 4). This trend was consistent across all materials; under oblique loading at a 30° load angle, zirconia's peak compressive stress rose from -185.47 MPa to -233.95 MPa, while leucite-reinforced porcelain increased from -176.29 MPa to -228.62 MPa when the load was concentrated at a single point (Table 4).

Interestingly, at this baseline temperature, the maximum principal stress values exhibited a slight decrease under combined loading compared to distributed loading, suggesting that at 22 °C, the point-load application primarily concentrates energy into compressive vectors. For example, in Leucite-reinforced porcelain subjected to vertical loading at 0°, the maximum tensile stress was 109.34 MPa with distributed loading and slightly decreased to 104.95 MPa under combined loading (Table 4). Despite these shifts in peak surface intensities, the average principal stress values remained remarkably stable across loading modes, indicating that the bulk of the material experiences the same global stress state. For zirconia at 22 °C under oblique loading (30°), the average maximum principal stress was 7.22 MPa for distributed loading and 7.11 MPa for combined loading, a negligible difference (Table 4). These findings underscore that at neutral oral temperatures, the primary effect of combined loading is the creation of localized compressive hot spots at the contact point, which increases the risk of surface damage without altering the overall mechanical demand on the crown's bulk.

### 3.2. Influence of Temperature and Load Angle

The finite element analysis showed that both environmental temperature and the angle of mechanical loading significantly influence stress patterns in ceramic crowns. The interaction between thermal expansion and mechanical constraints creates distinct stress intensification patterns. Temperature was a key factor affecting stress magnitude. Using 22°C as a baseline, increasing the temperature to 70°C or decreasing it to 5°C led to higher internal stresses across all materials, with 70°C producing the highest stresses. For zirconia, the maximum principal stress under an oblique load (30°) increased from 129.11 MPa at 22°C to 184.89 MPa at 70°C, a roughly 43% rise (Table 4, Figure 2). Lowering the temperature to 5°C also caused notable thermal stresses, but generally less than at 70°C. For instance, lithium disilicate's maximum principal stress under oblique load (30°) for distributed loading was 128.35 MPa at 5°C, slightly higher than 126.91 MPa at 22°C (Table 4, Figure 2).

Shifting from vertical (0°) to oblique (30°) loading consistently increased both tensile and compressive stresses across all material types, reflecting the more complex biomechanical forces

encountered during lateral mandibular movements. For example, under a 70 °C thermal load and distributed mechanical loading, the maximum principal stress for lithium disilicate rose from 117.42 MPa at a 0° angle to 129.36 MPa at 30°(Table 4, Figure 2). Similarly, the magnitude of the minimum principal stress was significantly higher at the oblique angle. For zirconia under 70

**Table 4. Maximum (tensile) and minimum (compressive) principal stresses throughout the molar tooth crown under compression load for different materials, loading, and thermal conditions.**

| Material | Temp. | Load angle | Loading condition | Max. Principal Stress (MPa) | | Min. Principal Stress (MPa) | |
|---|---|---|---|---|---|---|---|
| | | | | Max. | Average | Max. | Average |
| Lithium disilicate | 5 °C | 0° | Applying a 450 N load by distributing it as 90 N loads to five surfaces. | 108.20 | 11.32 | -156.43 | -11.39 |
| | | 30° | | 128.35 | 15.23 | -180.45 | -12.34 |
| | 22 °C | 0° | | 109.09 | 2.75 | -158.38 | -10.01 |
| | | 30° | | 126.91 | 7.38 | -181.99 | -11.70 |
| | 70 °C | 0° | | 117.42 | 7.84 | -199.80 | -34.70 |
| | | 30° | | 129.36 | 10.90 | -239.40 | -35.32 |
| | 5 °C | 0° | Applying a load of 450 N to five surfaces as a single, combined force. | 103.83 | 11.29 | -190.65 | -11.54 |
| | | 30° | | 123.07 | 15.15 | -223.43 | -12.45 |
| | 22 °C | 0° | | 104.78 | 2.71 | -199.94 | -10.16 |
| | | 30° | | 121.65 | 7.28 | -232.25 | -11.84 |
| | 70 °C | 0° | | 113.27 | 7.81 | -249.69 | -34.88 |
| | | 30° | | 124.38 | 10.84 | -304.35 | 35.50 |
| Zirconia | 5 °C | 0° | Applying a 450 N load by distributing it as 90 N loads to five surfaces. | 119.46 | 24.62 | -158.27 | -15.21 |
| | | 30° | | 151.47 | 28.10 | -182.79 | -15.63 |
| | 22 °C | 0° | | 108.49 | 2.50 | -161.76 | -10.02 |
| | | 30° | | 129.11 | 7.22 | -185.47 | -11.71 |
| | 70 °C | 0° | | 184.18 | 20.22 | -316.87 | -74.37 |
| | | 30° | | 184.89 | 22.92 | -332.01 | -74.14 |
| | 5 °C | 0° | Applying a load of 450 N to five surfaces as a single, combined force. | 104.32 | 24.55 | -184.99 | -15.37 |
| | | 30° | | 134.17 | 28.02 | -217.01 | -15.75 |
| | 22 °C | 0° | | 104.27 | 2.43 | -202.50 | -10.18 |
| | | 30° | | 123.79 | 7.11 | -233.95 | -11.85 |
| | 70 °C | 0° | | 184.35 | 20.21 | -346.46 | -74.64 |
| | | 30° | | 184.81 | 22.89 | -396.4 | -74.45 |
| Leucite-reinforced feldspathic porcelain | 5 °C | 0° | Applying a 450 N load by distributing it as 90 N loads to five surfaces. | 108.75 | 12.28 | -149.86 | -11.64 |
| | | 30° | | 125.35 | 15.99 | -174.23 | -12.51 |
| | 22 °C | 0° | | 109.34 | 3.25 | -152.42 | -10.12 |
| | | 30° | | 123.48 | 7.68 | -176.29 | -11.81 |
| | 70 °C | 0° | | 117.31 | 8.28 | -203.62 | -35.66 |
| | | 30° | | 125.37 | 11.31 | -247.29 | -36.38 |
| | 5 °C | 0° | Applying a load of 450 N to five surfaces as a single, combined force. | 120.18 | 15.97 | -217.52 | -12.64 |
| | | 30° | | 124.35 | 12.31 | -226.23 | -12.81 |
| | 22 °C | 0° | | 104.95 | 3.27 | -193.67 | -10.28 |
| | | 30° | | 118.34 | 7.63 | -228.62 | -11.95 |
| | 70 °C | 0° | | 113.14 | 8.25 | -250.88 | -35.85 |
| | | 30° | | 120.57 | 11.27 | -308.93 | -36.55 |

°C combined loading, the peak compressive stress reached -396.4 MPa at 30°, compared to -346.46 MPa at 0° (Table 4, Figure 3).

The most critical scenario for all materials was the combination of 70°C temperature and a 30° loading angle. As shown in Figure 4, the tensile stresses at 70°C/30° were primarily concentrated at the occlusal contact points and the cervical margins. Zirconia displayed the most intense hot zones (red/orange) compared to the lithium disilicate and leucite-reinforced feldspathic porcelains. Figure 5 illustrates that compressive stresses were highly localized at the specific points of load application on the five surfaces. The 30° angle shifted the stress distribution deeper into the crown structure, particularly visible in the zirconia model (Fig. 5B), where the compressive zones (blue/purple) reached their maximum magnitudes.

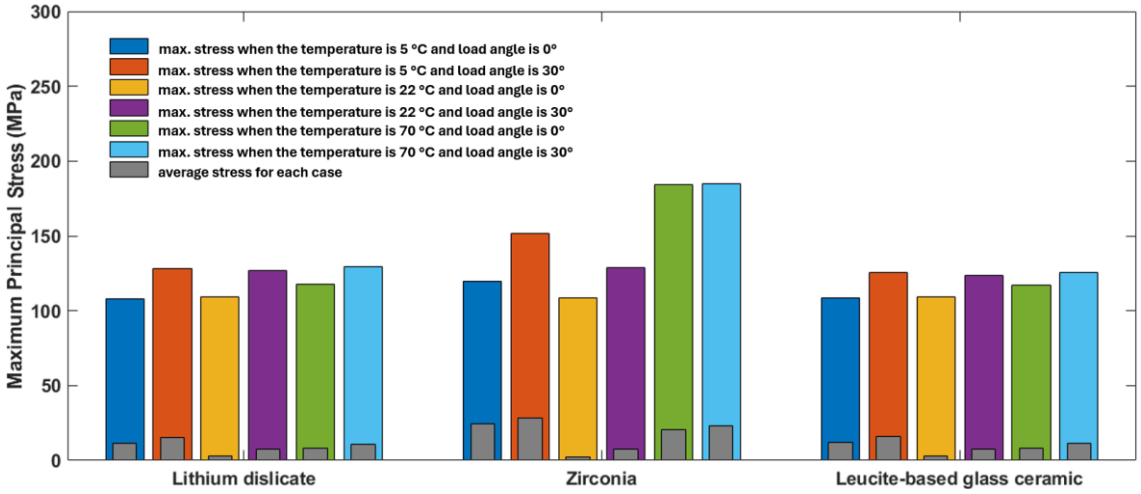


***Figure 2:***
*Maximum principal stresses for various dental crown materials under distributed loading*

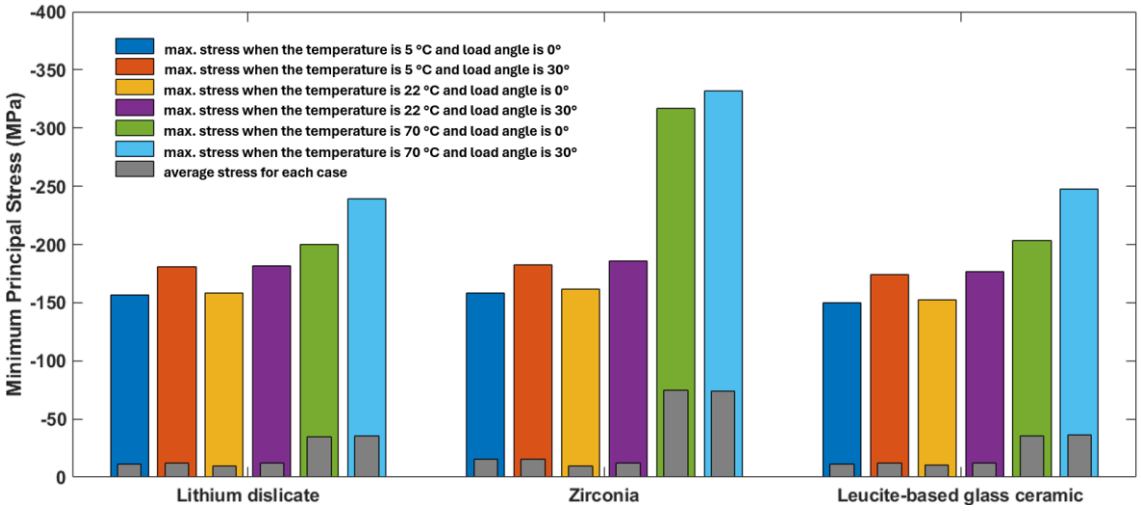


***Figure 3****:*
*Minimum principal stresses for various dental crown materials under distributed loading*

Temperature and loading angles are known to influence the mechanical behavior of dental ceramics because of their brittle nature and temperature-sensitive microstructure (Uppangala et al., 2023). In the present study, increasing the temperature and load angle resulted in higher maximum and minimum principal stress values across all investigated materials and loading conditions. This trend was more pronounced in stiffer, more brittle materials, indicating greater

sensitivity to thermomechanical loading. As temperature increases, thermal expansion mismatch within the material may promote stress redistribution and localized deformation, contributing to elevated stress levels. Similarly, increasing the load angle to 30° introduces a shear component to the applied load, which leads to higher stress development compared with purely axial loading (0°).

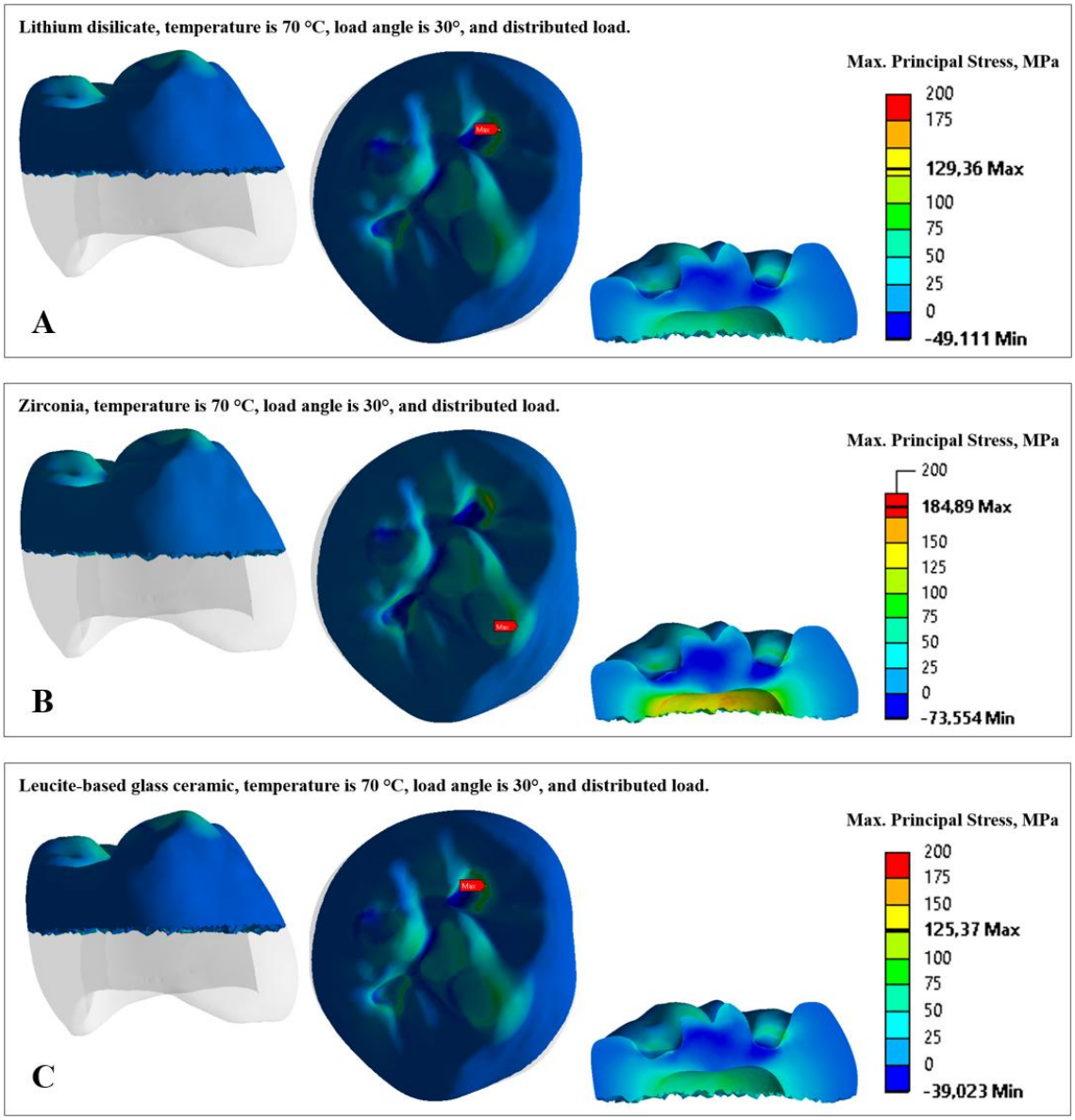


***Figure 4:***
*Maximum principal stress distributions for a dental crown under thermal (70 °C) and loading conditions (load angle is 30° and load was distributed) for A) lithium disilicate, B) zirconia, and C) leucite-reinforced feldspathic porcelain.*

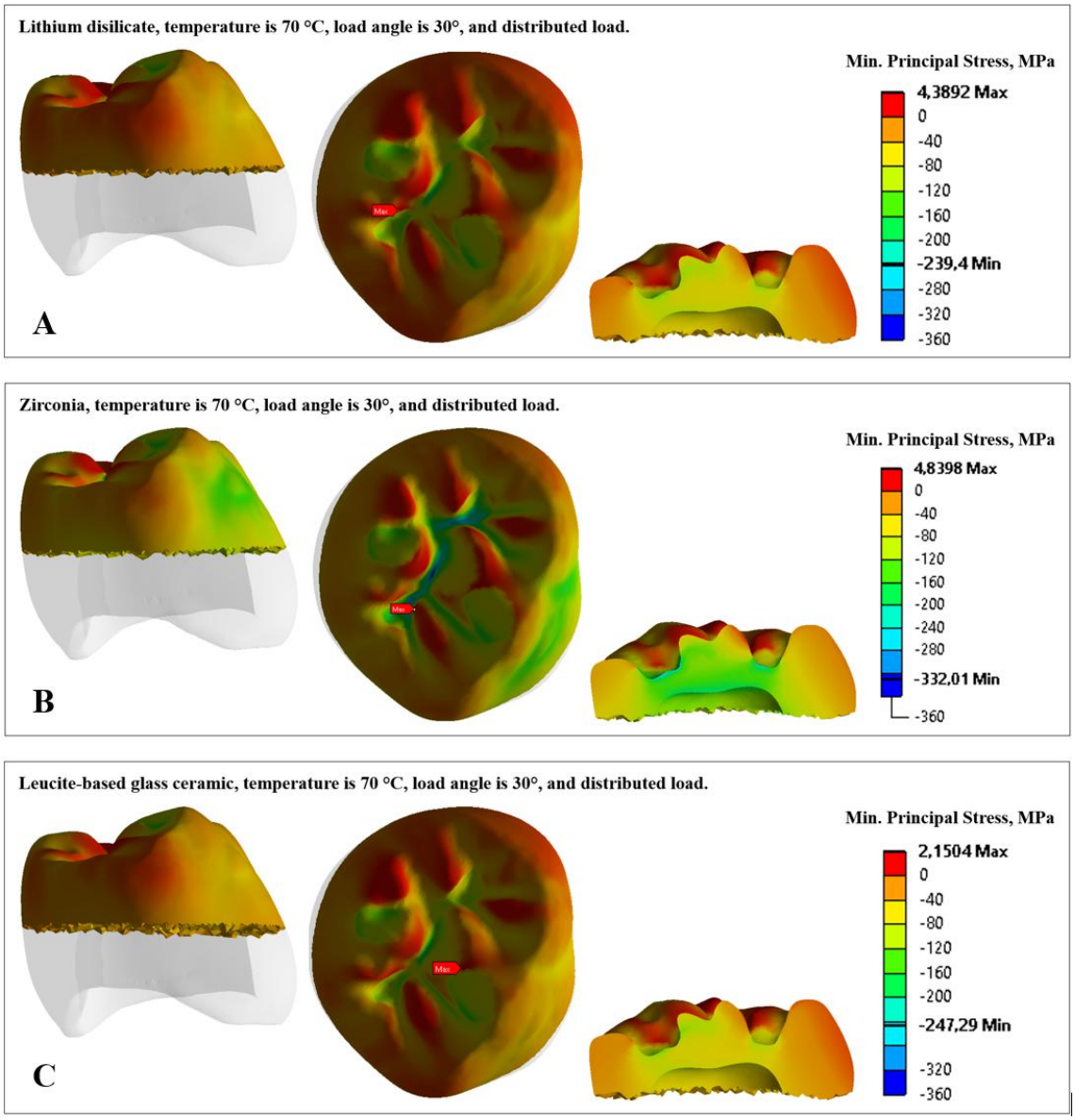


***Figure 5:***
*Minimum principal stress distributions for a dental crown under thermal (70 °C) and loading conditions (load angle is 30° and load was distributed) for A) lithium disilicate, B) zirconia, and C) leucite-reinforced feldspathic porcelain..*

### 3.3. Effect of Load Distribution Method

Beyond thermal and angular variables, the method of load application (distributed versus combined) played a decisive role in localizing compressive stress concentrations. While maximum principal stress remained relatively stable, the single-point combined load (450 N) consistently generated higher peak compressive (minimum principal) stresses than the distributed scenario. For instance, at 70°C and a 30° load angle, the magnitude of minimum principal stress in zirconia intensified from -332.01 MPa under distributed loading to -396.4 MPa when the load was combined into a single force (Table 4).

A similar trend was observed in the compressive stress for lithium disilicate, which increased from -239.40 MPa (distributed) to -304.35 MPa (combined) at 70°C and 30°. This pattern of intensification remained consistent even at the lower temperature extremes; for example, at 5°C and a 0° angle, leucite-reinforced porcelain exhibited a maximum stress of 120.18 MPa under combined loading compared to 108.75 MPa under distributed loading. These findings confirm that localized, single-point application of force results in non-physiological stress concentrations that significantly reduce the restoration's safety margin compared to more realistic, distributed occlusal contacts

We found that the minimum principal stresses on the dental crown under a combined single compressive load increased compared to the distributed load (Table 4, Figures 2, 3). Constantino et al. explored that multi-cusp teeth resist bite forces better when multiple cusps contact simultaneously, distributing load more evenly and reducing stress concentration (Constantino et al., 2016). A similar XFEM-based FEA by Ni et al. (2023) showed that internal stress concentrations depend heavily on occlusal loading patterns—distributed lateral and vertical loads result in different stress distributions and crack initiation thresholds. Our findings, consistent with previous studies (Constantino et al., 2016; Ni et al., 2023), suggest that distributed occlusal contacts, such as those from multiple cusps or food particles, may lead to broader internal stress development compared to concentrated forces. This could impact failure mechanisms like crack propagation and chipping in clinical settings.

### 3.4. Structural Integrity and Failure Risk Analysis

Although zirconia exhibited the highest stress levels due to its high modulus of elasticity, it demonstrated the greatest structural success. With a flexural strength of 900 MPa (Table 3) (Al Mortadi et al., 2020), and a peak maximum principal stress value of 184.89 MPa (under 70°C and 30° distributed loading) (Table 4), the material utilized only 20.5% of its maximum capacity. Even under the most taxing condition (combined Load at 70°C/30°), where the maximum principal stress reached 184.81 MPa (Table 4), zirconia maintained a safety factor of approximately 4.87, significantly exceeding the 4.0 threshold.

Lithium disilicate showed a robust performance. At a peak tensile stress of 129.36 MPa (70°C, 30° distributed load) (Table 4), it reached approximately 36.2% of its 356.7 MPa (Table 3) (Al Mortadi et al., 2020) flexural strength. This suggests a high degree of clinical reliability for both anterior and posterior applications under standard chewing forces.

This material exhibited the lowest safety margin. While its peak maximum principal stress value was numerically similar to lithium disilicate (125.37 MPa at 70°C, 30° distributed load) (Table 4), its lower flexural strength of 160 MPa (Table 3) (https://ivodent.hu/__docs/775_d9ea1b27d845c2dd50ef19b4a86c1fdc.pdf) means it was subjected to 78.3% of its failure threshold. Under these extreme thermal and mechanical conditions, the material operates near its mechanical limit, indicating a risk of fracture compared to the other two ceramics.

### 3.5. Comparative Material Behavior

A comprehensive evaluation of the three dental ceramics demonstrates that material selection is the primary determinant of a restoration's long-term mechanical success under thermal and mechanical loads. By synthesizing the maximum principal stress peaks, safety margins relative to flexural strength, and thermal expansion coefficients (Table 5), the materials can be ranked based on their robustness in a simulated oral environment.

The superior ranking of zirconia is supported by its exceptional flexural strength of 900 MPa, which provides a substantial safety factor of 4.87 (Table 5). Despite experiencing the highest stress concentrations (184.89 MPa) due to its high Young’s modulus of 210 GPa, its structural

integrity remains uncompromised, utilizing only approximately 20.5% of its total mechanical capacity. This confirms zirconia as the most reliable choice for posterior restorations where masticatory forces are highest and often oblique.

**Table 5. Comparative evaluation of dental crowns based on mechanical performance under thermal and mechanical loading conditions**

| Material | Flexural Strength ($\sigma_f$) | Max. Principal Stress ($\sigma_{max}$) | Safety Factor ($\sigma_f$ / $\sigma_{max}$) | Thermal Stress Sensitivity (CTE) |
|---|---|---|---|---|
| Zirconia | 900 MPa | 184.89 MPa | 4.87 | $10.8 \times 10^{-6}$ $K^{-1}$ |
| Lithium disilicate | 356.7 MPa | 129.36 MPa | 2.76 | $10.6 \times 10^{-6}$ $K^{-1}$ |
| Leucite-reinforced feldspathic porcelain | 160 MPa | 125.37 MPa | 1.28 | $17.5 \times 10^{-6}$ $K^{-1}$ |

Lithium disilicate maintains a balanced profile, offering a flexural strength of 356.7 MPa and a calculated safety factor of 2.76 under peak loading conditions (Table 5). Its thermal stability is particularly noteworthy; with a coefficient of thermal expansion (CTE) of $10.6 \times 10^{-6}$ $K^{-1}$, it exhibits significantly lower thermal sensitivity than leucite-based alternatives (Table 5). This alignment results in more predictable stress distributions across varying temperatures, justifying its rank as a versatile material for both aesthetic and functional demands.

Conversely, leucite-reinforced feldspathic porcelain is ranked third due to its narrow safety margins. With the lowest flexural strength (160 MPa) and the highest CTE ($17.5 \times 10^{-6}$ $K^{-1}$), this material operates with a safety factor of only 1.28 (Table 5). Under the synergistic effects of high temperature (70 °C) and oblique loading (30°), the material functions near its failure threshold. The high thermal sensitivity and localized stress concentrations of 125.37 MPa significantly increase the probability of micro-crack formation (Table 5). These results suggest that while leucite-based ceramics offer high aesthetic value, they require precise clinical application to avoid exceeding their limited mechanical tolerances.

## 4. CONCLUSION

This study utilized finite element analysis to quantify stress dynamics in three dental ceramic crowns under varying thermal and mechanical conditions. The results demonstrate that restoration integrity is a synergistic function of environmental temperature, loading angle, and intrinsic material properties. Zirconia emerged as the most robust material; despite exhibiting the highest internal stresses, its superior flexural strength provides a critical safety buffer against intensification from extreme temperatures and oblique forces, making it ideal for high-load posterior applications. Conversely, leucite-reinforced porcelain operates near its mechanical failure threshold under extreme conditions, such as 70°C and 30° loading, due to its lower flexural strength and high thermal sensitivity. The analysis highlights the impact of loading geometry and thermal stability on prosthetic longevity. The transition from axial to oblique loading and the concentration of force into single combined loads significantly increase localized hot spots at occlusal contact areas and cervical margins, which are primary sites for micro-crack initiation. Furthermore, significant stress elevation at 70°C confirms that dietary thermal fluctuations act as major catalysts for material fatigue.

## CONFLICT OF INTEREST

The authors confirm that there are no known conflicts of interest or shared interests with any organization, institution, or individual.

## AUTHOR CONTRIBUTION

Murat HORASAN: Conceptualization, formal analysis, investigation, methodology, supervision, visualization, writing – original draft, writing – review and editing.

Murat ŞENOL: Conceptualization, investigation, methodology, writing – original draft, writing – review and editing.

## REFERENCES


**1.** Al-Maqtari, A. A., Razak, A. A. A., & Hamdi, M. (2014) 3D finite element analysis of functionally graded multilayered dental ceramic cores, *Dental Materials Journal*, 33(4), 458–465. doi:10.4012/dmj.2013-251

**2.** Al Mortadi, N., Bataineh, K., & Al Janaideh, M. (2020) Fatigue failure load of molars with thin-walled prosthetic crowns made of various materials: A 3D-FEA theoretical study, *Clinical, Cosmetic and Investigational Dentistry*, 12, 581–593. doi:10.2147/CCIDE.S286826

**3.** Ayatollahi, M. R., Yahya, M. Y., Karimzadeh, A., Nikkhooyifar, M., & Ayob, A. (2015) Effects of temperature change and beverage on mechanical and tribological properties of dental restorative composites, *Materials Science and Engineering C*, 54, 69–75. doi:10.1016/j.msec.2015.05.004

**4.** Benazzi, S., Nguyen, H. N., Kullmer, O., Kupczik, K. (2016) Dynamic Modelling of Tooth Deformation Using Occlusal Kinematics and Finite Element Analysis. *PLoS ONE*, 11(3), e0152663. doi:10.1371/journal.pone.0152663

**5.** Capobianco, V., Baroudi, K., Santos, M. J. M. C., Rubo, J. H., Rizkalla, A. S., de Oliveira Dal Piva, A. M., Vitti, R. P., Tribst, J. P. M., & Santos, G. C. (2023) Post-fatigue fracture load, stress concentration and mechanical properties of feldspathic, leucite- and lithium disilicate-reinforced glass ceramics, *Heliyon*, 9(7), e17787. doi:10.1016/j.heliyon.2023.e17787

**6.** Constantino, P. J., Bush, M. B., Barani, A., & Lawn, B. R. (2016) On the evolutionary advantage of multi-cusped teeth, *Journal of the Royal Society Interface*, 13(121), 20160374. doi:10.1098/rsif.2016.0374

**7.** Cuzic, C., Rominu, M., Pricop, A., Urechescu, H., Pricop, M. O., Rotar, R., Cuzic, O., Sinescu, C., & Jivanescu, A. (2025) Clinician's guide to material selection for all-ceramics in modern digital dentistry, *Materials*, 18(10), 2235. doi:10.3390/ma18102235

**8.** da Mota Fonseca, L. C., Faé, D. S., Fernandes, B. N., da Costa, I., Miranda, J. S., & Lemos, C. A. A. (2025) Are implant-supported monolithic zirconia single crowns a viable alternative to metal-ceramics? A systematic review and meta-analysis, *Ceramics*, 8(2), 63. doi:10.3390/ceramics8020063

**9.** Di Francesco, P., Bechir, A., Popescu, A. I., Chivu, M. V., Dobrescu, A. M., Comăneanu, R. M., & Târcolea, M. (2025) Finite element analysis (FEA) of the stress behavior of some dental materials, *Journal of Medicine and Life*, 18(1), 29–37. doi:10.25122/jml-2025-0005

**10.** Edmonds, H. M., & Glowacka, H. (2020) The ontogeny of maximum bite force in humans, *Journal of Anatomy*, 237(3), 529–542. doi:10.1111/joa.13218

**11.** Fehrenbach, J., de Soares, J. L. S., do Nascimento Foly, J. C. S., Miotti, L. L., & Münchow, E. A. (2025) Mechanical performance of endocrown restorations in anterior teeth: A systematic review and network meta-analysis, *Dental Materials*, 41(1), 28–41. doi:10.1016/j.dental.2024.10.012

**12.** Gongal, D., Thakur, S., Panse, A., Shankarrao, P., Stark, J. A., Hetling, J. R., Ozgen, B., & Foster, C. D. (2023) Thermal finite element analysis of localized hypothermia treatment of the human eye, *Medical Engineering & Physics*, 111, 103928. doi:10.1016/j.medengphy.2022.103928

**13.** Hannigan, A., & Lynch, C. D. (2013) Statistical methodology in oral and dental research: Pitfalls and recommendations, *Journal of Dentistry*, 41(5), 385–392. doi:10.1016/j.jdent.2013.02.013

**14.** Ivoclar Vivadent AG. Scientific documentation IPS Empress CAD. (https://ivodent.hu/__docs/775_d9ea1b27d845c2dd50ef19b4a86c1fdc.pdf) (Accessed July 23, 2025)

**15.** Lahoud, P., Faghihian, H., Richert, R., Jacobs, R., & EzEldeen, M. (2024) Finite element models: A road to in-silico modeling in the age of personalized dentistry, *Journal of Dentistry*, 150, 105348. doi:10.1016/j.jdent.2024.105348

**16.** Marrelli, M., Pujia, A., Apicella, D., Sansalone, S., & Tatullo, M. (2015) Influence of peak oral temperatures on veneer-core interface stress state, *Acta Biomaterialia Odontologica Scandinavica*, 1(1), 22–28. doi:10.3109/23337931.2015.1039536

**17.** Miranda, N. C. F., Gialain, I. O., Gantier-Takano, M. K., Ballester, R. Y., Hernandez, B. A., Fok, A., & Meira, J. B. C. (2025) Should the load-to-fracture test for CAD/CAM monolithic molar crowns be standardized, and how? A systematic review and finite element analysis, *Journal of the Mechanical Behavior of Biomedical Materials*, 168, 106984. doi:10.1016/j.jmbbm.2025.106984

**18.** Ni, J., Xu, L., Lin, Y., Lai, D., & Huang, X. (2023) Effects of different full-coverage designs and materials on crack propagation in first mandibular molar: An extended finite element method study, *Frontiers in Bioengineering and Biotechnology*, 11, 1222060. doi:10.3389/fbioe.2023.1222060

**19.** Sasany, R., Saraç, D., & Özcan, M. (2021) Effect of different liner techniques and argon plasma treatment of zirconia based on the adhesion and color change of veneering ceramic, *Journal of Adhesion Science and Technology*, 35(18), 1981–1994. doi:10.1080/01694243.2020.1869398

**20.** Trivedi, S. (2014) Finite element analysis: A boon to dentistry, *Journal of Oral Biology and Craniofacial Research*, 4(3), 200–203. doi:10.1016/j.jobcr.2014.11.008

**21.** Uppangala, R. S., Pai, S., Patil, V., Smriti, K., Naik, N., Shetty, R., Gunasekar, P., Jain, A., Tirupathi, J., Hiremath, P., Patil, S., & Rathnakar, R. (2023) Influence of thermal and thermomechanical stimuli on dental restoration geometry and material properties of cervical restoration: A 3D finite element analysis, *Journal of Composites Science*, 7(1), 6. doi:10.3390/jcs7010006

**22.** Valandro, L. F., Özcan, M., Amaral, R., Vanderlei, A., & Bottino, M. A. (2008) Effect of testing methods on the bond strength of resin to zirconia-alumina ceramic: Microtensile versus shear test, *Dental Materials Journal*, 27(6), 849–855. doi:10.4012/dmj.27.849

**23.** Weinstein, C., Hirschhaut, M., Flores-Mir, C. (2025) Occlusal adjustment in the digital era – A working protocol, Seminars in Orthodontics, 31(1), 18-46, doi:10.1053/j.sodo.2024.11.003.

**24.** Zarone, F., Di Mauro, M. I., Ausiello, P., Ruggiero, G., & Sorrentino, R. (2019) Current status on lithium disilicate and zirconia: A narrative review, *BMC Oral Health*, 19(1), 134. doi:10.1186/s12903-019-0838-x